京都大学防災研究所年報 第 60 号 B 平成 29 年
DPRI Annuals, No. 60 B, 2017

Numerical Simulation of River Bed Deformation due to Unsteady Flow of Large Sand-Bed Braided River: Brahmaputra-Jamuna

SHAMPA (1), Yuji HASEGAWA, Hajime NAKAGAWA, Hiroshi TAKEBAYASHI and Kenji KAWAIKE

(1) Department of Civil and Earth Resources Engineering, Graduate School of Engineering, Kyoto University

Synopsis

Numerous bars and channels are an essential large scale topographic feature of the braided river morphology. During the monsoon season, due to the unsteady change in hydrograph, these bars and channels experience simultaneous reworking which is quite uncertain. Through this study, we reproduced the river bed deformation due to unsteady flow which generally happens during the monsoon season using numerical simulation. Along with this, we tried to investigate some individual bar scale property as well as their interaction with the braided plain of a highly sediment-laden reach of Brahmaputra-Jamuna River. Our study indicates that the frequency of deposition on the river bed or braided plain was higher compared to the erosion due to the response of unsteady discharge and water level change in the study reach. Nevertheless, the development process of the braided bars is quite different from the bars of straight and meandering channels. The spatial growth of the bar seems to be dependent on the width-depth ratio up to a certain limit and finally, the migration rate of the bar recedes with the growth of the bar.

Keywords: Braided River, bed deformation, bar dynamics, Delft3D, Migration rate

1. Introduction

Networks of channels separated by transient bars exemplify the uniqueness of braided type of river. During the monsoon season, due to the high flow, the change of plan-form becomes very rapid and unpredictable especially in the case of sand bed one due to relatively high energy and intense bedload dominated transport condition which accelerates instability to the entire network (Ashmore, 2013; Egozi et al., 2009). During the monsoon season when the heavy flow comes, the entire network may be submerged or partly which adds difficulties to predict the networks especially the growth of the mid-channel bars (Kleinhans and van den Berg, 2011; Schuurman et al., 2013). In case of highly sediment-laden river, as the growth of these bars is not unidirectional; several bars may rejoin or dissects during that period (Sarker el al., 2003; ISPAN; 1993, Schuurman et al., 2013).

Moreover, in highly sediment-laden braided river different types of bars are found like unit bar or compound bar (based on formation type) and free bars or force bars (according to forcing). The linear bar theory clarifies the relationship between bar dimensions and channel geometry which is confirmed by many laboratory experiments, field observations, and mathematical analyses but in case of highly sediment driven braided river which contains so many compound bar; applicability of

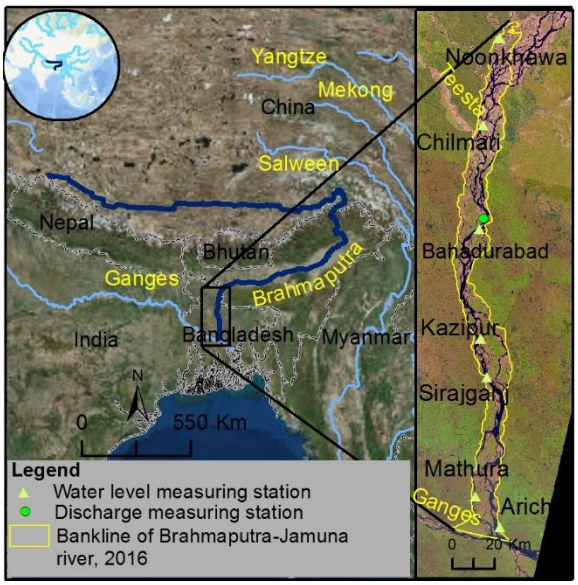

Figure 1: Map showing the study area

such theory may not be fully successful every time (Muramoto and Fujita, 1978; Colombini et al., 1987; Ikeda, 1990; Yalin, 1992; Garcia and Nino, 1993; Schuurman et al., 2013). Nevertheless, the interaction of compound bar and unit bar with the braid plain is poorly understood (Kleinhans and van den Berg, 2011; Schuurman et al., 2013). Some researcher (Sarker el al., 2003; ISPAN; 1993) used satellite imagery analysis to understand this type of interaction but still there remains the need for clarifying the relation between the river hydraulic property and bar dynamics and in this case two-dimensional numerical simulations can be used as a tool for proper understanding of the river behavior.

Hence, the main objective of this research is to assess the deformation of river bed due to unsteady flow in monsoon season by numerical simulation. Attention was given to the spatial growth of bar by focusing their migration rate. Special attention was given to understand the relationship of geometrical properties of bar and channel during the alteration of flow.

As the study area, 225 km reach of Brahmaputra- Jamuna (downstream continuation of the Brahmaputra River in Bangladesh, see Figure 1) was selected. The river is well known for her extremely dynamic nature, with high sediment transport rate, 550 m ton/y (Delft Hydraulics and DHI; 1996, Baki and Gan, 2012; Sarker et al., 2014). The morphological features of the river (bars and channels) experience major changes in area, shape and spatial distribution each year to respond the pulsation of discharge and sediment load during the flood (annual fluctuation of discharge is more than 60,000 m^3/s) (Sarker et al., 2014).

2 Methodology

2.1 General approach

As like as the other sand bed braided river, compound bars are more common in this reach compared to the unit bars. The growth of unit bar is comparatively straightforward compared to the compound bar which can migrate upstream, downstream even laterally by being collated with other bars (Bridge, 1993). Hence the planform changes of the river become very unpredictable due to these dynamic characteristics of these bars. Therefore, to understand these dynamics; in this study, we developed a 2D morphodynamic model by incorporating the real river bathymetry and boundary condition for the year 2011 using Delft3D software and simulated for one monsoon period from- 1st of June, 2011 to 15th of October, 2011. The assumption works behind this was the major morphological changes for that particular year occurred within the peak discharge period of the hydrograph. The model was well calibrated and validated for the year 2012. Then, we have calculated some bar scale property and tried to develop the relationship with the river hydraulic property.

In addition to this, we defined and calculated the migration rate of the compound bars. As the growth of the compound mid-channel bar is not unidirectional; merging of two or three bars during the high flood is very common, we consider the highest lateral distance from the old one to newly developed one in a particular direction as the migration amount/celerity of that particular bar for that particular year (details can be seen in Shampa et al., 2017)

2.2 Bar Properties

Definitions used by previous researchers by defining bar properties were followed here especially Garcia and Nino (1993), Schuurman et al. (2013) and Eaton and Church (2011). For

determining bar length, one bar was treated as individual object and the longest axis gives the length of the bar, L and the difference between trough and crest gives the value of bar amplitude, H. For dimensional analysis, dimensionless bar height Hb was calculated by dividing Bar amplitude H by the maximum scour depth S_o, $Hb=H/S_o$. Constant channel width, W was considered and river's width/depth, β is defined by dividing this width by the maximum water depth d. The value of celerity of bar to is the mean flow velocity, *U* shows the relative migration rate, ω. Aspect ratio, α is defined by the bar length to width ratio. The dimensionless stream power **Ω*** was calculated by

$$\Omega^* = \frac{gdSU_0}{[gRD_{50}]^{3/2}} \quad (1)$$

Here g is gravitational acceleration, S defines slope and R is the submerged sp. gravity of sediment.

2.3 Description of 2D Model

A two-dimensional depth average morphodynamic model was developed using Delft3D software (version 4.00.01) by applying the following hydrodynamic equations.

Conservation of mass was calculated by using the continuity equation:

$$\frac{\partial \eta}{\partial t} + \frac{\partial (du)}{\partial x} + \frac{\partial (dv)}{\partial y} = 0 \quad (2)$$

In x-direction conservation of momentum:

$$\frac{\partial u}{\partial t} + u\frac{\partial u}{\partial x} + v\frac{\partial u}{\partial y} + g\frac{\partial \eta}{\partial x} + \frac{gu|U|}{C^2 d} - v_t\left(\frac{\partial^2 u}{\partial x^2} + \frac{\partial^2 u}{\partial y^2}\right) + F_x = 0 \quad (3)$$

In y-direction conservation of momentum:

$$\frac{\partial v}{\partial t} + u\frac{\partial v}{\partial x} + v\frac{\partial v}{\partial y} + g\frac{\partial \eta}{\partial y} + \frac{gv|U|}{C^2 d} - v_t\left(\frac{\partial^2 v}{\partial x^2} + \frac{\partial^2 v}{\partial y^2}\right) + F_y = 0 \quad (4)$$

Where

η = water level elevation (here in m)

d = water depth (m)

u,v =velocity in the x- and y-directions, respectively (m/s)

U = magnitude of total depth-averaged velocity (m/s)

$F_{x,y}$=x and y components of external forces

g= acceleration due to gravity (m/s^2)

ρ =water density (kg/m^3)

v_t =eddy viscosity (m^2/s)

C =Chézy coefficient ($m^{1/2}/s$)

Kabir and Ahmed (1996) compared different sediment transport formulae using field data (collected by Flood Action Plan -24) and concluded that Van Rijn (1984) estimates well peak period sediment discharge (Figure 2).

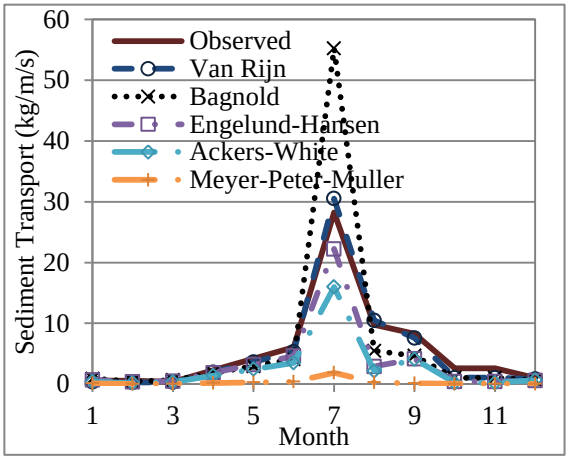

Figure 2: Comparison between observed and estimated Sediment load of Jamuna River (Kabir and Ahmed; 1996)

Therefore, we also adopted this formula for estimating sediment discharge considering equilibrium sand concentration at inflow boundary. The total load, qθ (Eq. (5) has been calculated using bed load transport qθb and suspended load transport qθs:

$$q\theta = q\theta b + q\theta s \quad (5)$$

The bed load transport rate qθb is computed by Eq.(6)

$$q\theta b = \begin{cases} 0.053\sqrt{\Delta g D_{50}^3}\, D_*^{-0.3}\left(\frac{\mu_c\tau - \tau_c}{\tau_c}\right)^{2.1} & if \left(\frac{\mu_c\tau - \tau_c}{\tau_c}\right) < 3.0 \\ 0.1\sqrt{\Delta g D_{50}^3}\, D_*^{-0.3}\left(\frac{\mu_c\tau - \tau_c}{\tau_c}\right)^{1.5} & if \left(\frac{\mu_c\tau - \tau_c}{\tau_c}\right) \geq 3.0 \end{cases} \quad (6)$$

The suspended load transport qθs is defined by Eq. (7)

$$q\theta s = f_s U d C_a \qquad (7)$$

Where, the dimensionless particle parameter is D*, τ_c =critical bed shear stress, and τ = bed shear stress and fs=shape factor for the vertical distribution of suspended sediment and Ca=reference concentration (VanRijn, 1984). Bed slope effect was considered for bed load transport and directional sediment transport derivatives q_x and q_y were calculated by using the following equations

$$q_x = q\theta b(\cos\phi_\tau - f(\theta)\frac{\partial \eta_b}{\partial x}) \qquad (8)$$

$$q_y = q\theta b(\sin\phi_\tau - f(\theta)\frac{\partial \eta_b}{\partial y}) \qquad (9)$$

Where, $$f(\theta) = \frac{1}{\varepsilon\theta^\beta} \qquad (10)$$

θ is the shield mobility parameter, ε and β is the calibration parameter and ϕ_τ is the angle between the flow direction and sediment transport vector and Δηb is changing in bed level is calculated by using Exner (1925) equation for conservation of mass for sediment calculated as following

$$\partial\eta_b/\partial t = MF(\frac{\Delta q_x}{\Delta x} + \frac{\Delta q_y}{\Delta y}) \qquad (11)$$

Here, MF is the Morphological acceleration factor.

2.4 Model Schematization

As the numerical model domain, 225 km long curvilinear grid was constructed with an average width of 13 km as shown in Figure 3.The model domain started from almost 10 km downstream from the Noonkhawa station and ended near Aricha, just upstream of the confluence with Ganges (Figure 3). The reach was discretized by 1117x73 grid cells. Such grid resolution was chosen to make a balance between computational time, the scale of the processes, and desired level of detail.

The simulation was carried out for 137 days from 1st of June, 2011 to 15th of October, 2011. The river Brahmaputra-Jamuna has only one discharge measuring station at Bahadurabad (Figure 3) which situates almost at the middle part of the

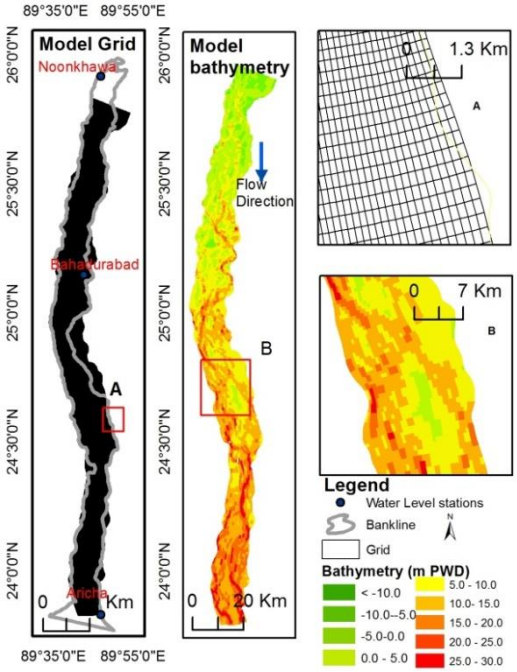

Figure 3: The model domain (Shampa et al., 2017)

study reach. However, there is one major contributing tributary of this river named as Teesta lies within the upper part of the study reach. Hence, for estimating the upstream boundary condition, the 1D model was used and the model was calibrated to the data at Bahadurabad. As the discharge data for Teesta, daily average time series data was used. As the downstream boundary, the water level data of Aricha of 2011 was used. The model boundary conditions are shown in Figure 4. Particle size (d_{50}) was assumed to be 277µm (Kabir and Ahmed, 1996).The specific density of sediment was 2650kg/m^3, hydrodynamic time step was 48 sec and morphodynamic time step was 144 sec. Constant Manning's roughness was used all over the domain and it was 0.027 s/($m^{1/3}$).

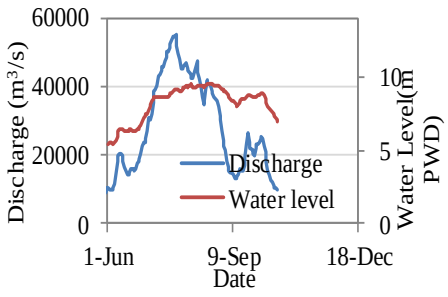

Figure 4: Boundary Condition of the model (Shampa et al., 2017)

2.5 Model Calibration and Validation

The water level calibration was done along four points Chilmari, Kazipur, Sirajganj and Mathura respectively while the discharge and sediment calibration were done only for Bahadurabad station (Locations are shown in Figure 1). Figure 5a and 5b shows the discharge, water level calibration result of the model at Bahadurabad and Mathura respectively. The calibration of sediment was done using the data set of sediment from 1968 to 2001 measured by BWDB and the data measured by Flood Action Plan 6, due to the lack of recent data as shown in Figure 5c. In this study, the model was verified for the hydraulic condition of the year 2012. The verification of the model for the water level at Sirajganj was shown in Figure 5d.

3 Results

3.1 Planform and bed deformation

The comparison between actual planform (planform of the river in 2012) and simulated one is shown in Figure 6a. This figure indicates that the model can predict the main anabranch but in the case of bar scale there are some discrepancies happens. As an example it could not predict well the alignment of chute channels. Figure 6b shows the time series bed level changes during the simulated period. As the model was simulated only for one peak season, not huge bed level change was observed except in some confluence; huge scour (like 23.66 m PWD in Sirajganj) was observed.

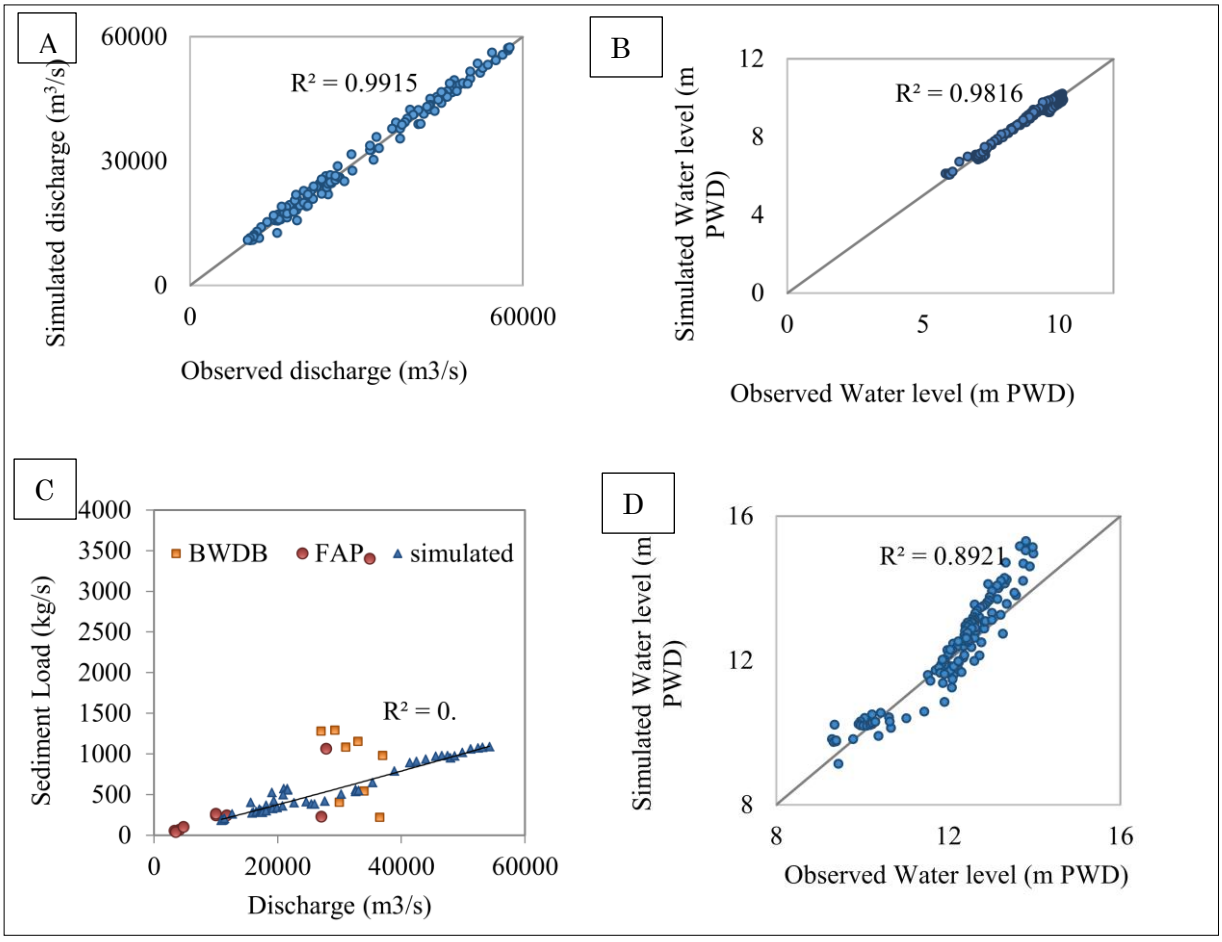

Figure 5: Calibration and validation of the model a): Discharge calibration: b) Water level calibration at Mathura c) Sediment calibration at Bahadurabad; d) Validation of the model for the year 2012 at Sirajganj.

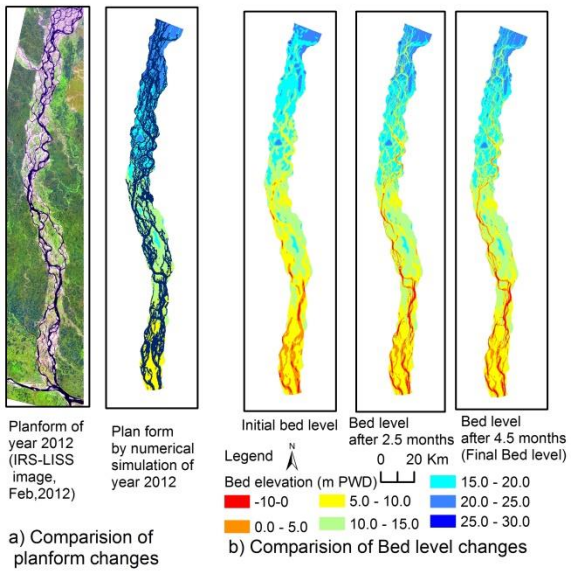

Figure 6: Comparison of real and simulated plan form and time series bed level change (reproduced from Shampa et al., 2017)

The histogram of bed elevation change is shown in Figure 7. This figure indicates the frequency of erosion and deposition in the simulated area and it shows that the maximum frequency of deposition is around 0 to 1m but 4m to 5m for erosion. The distribution bed level change is not evenly distributed. The reason behind this uneven distribution is the occurrence of large scour hole only at confluences and the confluences were not evenly distributed in the simulated reach.

The comparison of bar migration rate derived from satellite image and simulation is shown in Figure 8. This figure reveals that the prediction of

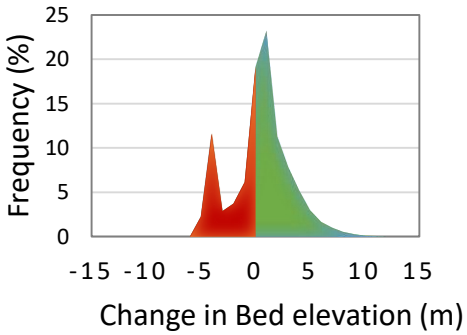

Figure 7: Histogram of bed level change (reproduced from Shampa et al., 2017)

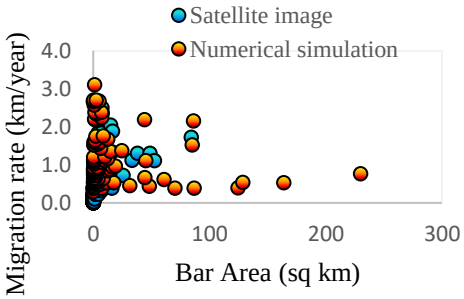

Figure 8: Comparison of bar migration rate derived from satellite image analysis and numerical simulation (Shampa et al., 2017)

spatial bar growth by simulation is comparable to the actual one. Both the simulation results and satellite imagery analysis showed the migration rate of bar recedes with the growth of bar. The higher migration (2-3km/year) rate observed when the bar is relatively small (the surface area was less than 50 sq km). The average migration rate of the bar is 1.05 km/year but satellite image analysis showed this rate was 0.04km/year. The reason for this discrepancy is that in the case of the satellite image analysis, the data is usually taken during the dry season (February), so from the end of monsoon to dry period the bars with the smaller area may experience some erosion.

3.2 Bar properties

The dimensionless Bar height and Bar length derived from the simulation result are plotted in Figure 9a and b. The results of the dimensionless Bar height, Hb analysis indicates that their good linear correlation width/depth ratio, β (Figure 9a).

But the dimensional less Bar length showed a nonlinear relationship with β and it seems there exists a critical value of L/W beyond this the bar do not elongate laterally. But the linear theory of bar indicates no such phenomenon for straight channel and meandering channels.

The relationship of dimensionless migration speed of bar with the function of width/depth ratio, β and bar aspect ratio, α and the dimensionless stream power, Ω* are shown in Figure 10a, b and c. This figure (Figure 10a and b) indicate that higher the depth of flow, lower the migration rate and

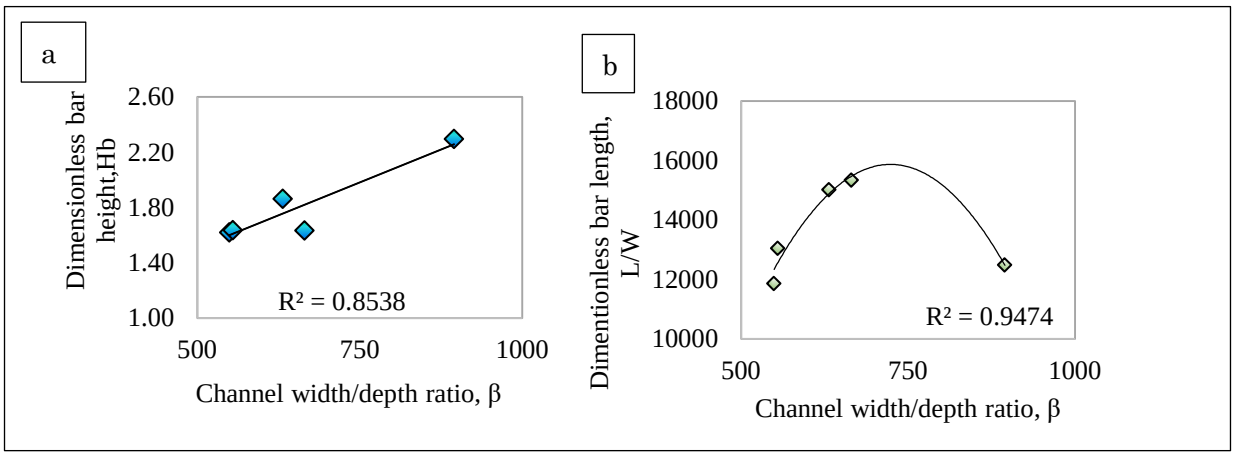

Figure 9: Relation between dimensionless width-depth ratios to a) dimensionless bar height b) dimensionless bar length (reproduced from Shampa et al., 2017)

migration rate also decreases with the increases in the bar area. Migration rate also decreased with the increase of channel stream power (Figure 10c).

4 Discussions and Conclusions

Through this study several phenomena of the braided bar has been investigated by using numerical simulation.

Doeschl et al (2009) and Ashmore (2013) showed the change of bed elevation of other braided river using physics-based model, laboratory experiment and field data and summarized the similar type distribution which we got in bed elevation change histogram shown in Figure 7. The rate of migration seems to be a little bit high compared with the previous researches; Bridge (1993) estimated this rate was 500 m per year. But they considered only one mid channel bar of Brahmaputra-Jamuna for their analysis.

bars in the straight channels or meandering one shown by Garcia and Nino (1993) but it indicates there may exist a critical point in case of dimensionless bar length.

The dimensionless migration rate of bar tends to decrease with the increase of bar area. These results indicate the bars in the upper part of the river are more unstable due to lower average depth. This phenomenon can be verified by many investigations (Sarker et al., 2003; ISPAN; 1993).Sarker et al. (2003). Egozi and Ashmore.(2008) Bertoldi et al.(2009) and Sarker et al. (2014) showed that the braiding intensity increases with the increasing discharge both for gravel bed and sand bed braided river and here the relationship of dimensionless migration rate and stream power also indicated that higher stream power is less favorable for the spatial growth of bar.

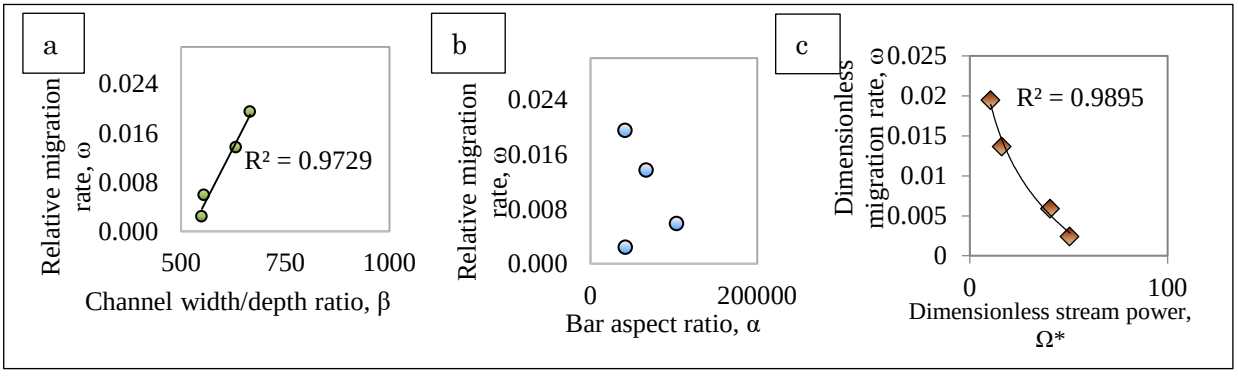

Figure 10: Relationship between a) Dimensionless migration speed to width-depth ratio b) Dimensionless migration speed aspect ratio and c) Dimensionless migration speed stream power

Based on our simulations and analysis, we concluded the following:

- Prediction of the complex growth of compound bar can be done using 2D morphodynamic model. But finer bathymetry data is needed for simulating some bar scale property (e.g. formation of chute channel over the bar).

- The frequency of deposition on the river bed or braided plain was higher compared to the erosion due to the response of unsteady change of discharge and water level change in the study reach of the Brahmaputra-Jamuna for that particular year.

- A migration rate of the bar naturally recedes with its growth. Hence, this phenomenon can also be used for better management of the braided river.

- The dimensionless bar property analysis indicates the spatial growth of braided bar can be skillfully controlled by controlling the width-depth ratio and channel discharge.

The next step of this research is to include the bank erosion process with the above mentioned model and estimate the effect of bar growth on bank erosion process.

Acknowledgements

The authors acknowledge JST-JICA funded SATREPS project "Research on Disaster Prevention/Mitigation Measures against Floods and Storm Surges in Bangladesh" for funding this research.

References

Ashmore, P. (2013): Morphology and dynamics of braided rivers. In: Shroder, J. (Editor in Chief), Wohl, E. (Ed.), Treatise on Geomorphology. Academic Press, San Diego, CA, Fluvial Geomorphology, Vol. 9, pp. 289–312.

Baki, A. B. M., & Gan, T. Y. (2012): Riverbank migration and island dynamics of the braided Jamuna River of the Ganges–Brahmaputra basin using multi-temporal Landsat images, Quaternary International, Vol.263, pp.148-161.

Bertoldi, W., Zanoni, L., & Tubino, M. (2009): Planform dynamics of braided streams, Earth Surface Processes and Landforms,Vol. 34(4), pp.547-557.

Bridge, J.S. (1993): The interaction between channel geometry, water flow, sediment transport and deposition in braided rivers. In: Braided Rivers (Eds Best, J.L. and Bristow, C.S.), Special Publication of the Geological Society of London, Vol. 75, pp.13–71.

Colombini, M., Seminara, G. and Tubino, M. (1987): Finite-amplitude alternate bars, J. Fluid Mech., Vol.181, pp. 213–232.

Delft Hydraulics and DHI. (1996): Floodplain levels and bankfull discharge, Special Report No. 6, River Survey Project (FAP 24)

Doeschl, A. B., Ashmore, P. E., & Davison, M. A. T. T.(2009): Methods for assessing exploratory computational models of braided rivers, Braided Rivers: Process, Deposits, Ecology and Management, International Association of Sedimentologists Special Publication, Vol.36, pp. 177-197.

Eaton, B. C., & Church, M. (2011): A rational sediment transport scaling relation based on dimensionless stream power, Earth Surface Processes and Landforms, Vol.36(7), pp.901-910.

Egozi R, Ashmore P. (2009): Experimental analysis of braided channel pattern response to increased discharge, Journal of Geophysical Research, vol, 114: pp.1-15.

Exner, F.M. (1925): On the interaction between water and sediment in rivers, Akad. Wiss. Wien Math. Naturwiss. Klasse, Vol. 134(2a), pp. 165-204.

Garcia, M. and Nino, Y.(1993): Dynamics of sediment bars in straight and meandering channels: experiments on the resonance phenomenon, J. Hydr. Res., Vol. 31(6), pp. 739–761.

Ikeda, S. (1990): Experiments by Engels on alternate bars. Summer School on Stability of River and Coastal Forms, La Colombella, Perugia, Italy, pp.3–14

ISPAN (FAP 16 and FAP 19) (1993): The Dynamic

Physical and Human Environment of Riverine Charlands: Jamuna, Dhaka, Bangladesh.

Kabir, M. R., & Ahmed, N. (1996): Bed shear stress for sediment transportation in the River Jamuna, Journal of Civil Engineering, The Institution of Engineers, Bangladesh Vol.CE24, pp.5568.

Kleinhans, M. G. and van den Berg, J. H. (2011): River channel and bar patterns explained and predicted by an empirical and a physics-based method. Earth Surf. Process. Landforms, Vol.36, pp. 721–738. doi:10.1002/esp.2090

Muramoto, Y. and Fujita,Y.A. (1978):Classification and formative conditions of river bed configuration of mesoscale, Proc. 22nd Japanese Conf. on Hydraulics, Japan Soc. Civ. Eng., pp. 275-282.

Sarker, M.H., Huque, I., Alam, M. and Koudstaal, R. (2003): Rivers chars and char dwellers of Bangladesh, International Journal River Basin Management, Vol. 1, pp 61-80.

Sarker, M. H., Thorne, C. R., Aktar, M. N., & Ferdous, M. R. (2014): Morpho-dynamics of the Brahmaputra–Jamuna River, Bangladesh. Geomorphology, Vol.215, pp.45-59.

Schuurman, F., Marra, W. A., & Kleinhans, M. G. (2013): Physics based modeling of large braided sandbed rivers: Bar pattern formation, dynamics, and sensitivity. Journal of Geophysical Research: Earth Surface, Vol.118 (4), pp. 2509-2527.

Shampa, Hasegawa Y., Nakagawa H., Takebayashi, H., Kawike, K. (2017): Dynamics of sand bars in braided river: a case study of Brahmaputra-Jamuna River, 自然災害科学 J. JSNDS 36 特別号, pp. 121-135. (Accepted)

Van Rijn, L.C.(1984). Sediment transport, Part I: Bed load transport, J. Hydraul. Eng., Vol. 110(10), pp.1431–1456. doi:10.1061/(ASCE)07339429(1984)110:10(143)

Yalin, M.S. (1992): River Mechanics, Pergamon Press, Oxford.

(Received June 13, 2017)